Low magnetic field depolarization of NV$^-$ centers through dipole-dipole interaction

C. Pellet-Mary[1], M. Perdriat[1], P. Huillery[?], G. Hétet[1]

[1] *Laboratoire De Physique de l'École Normale Supérieure, École Normale Supérieure, PSL Research University, CNRS, Sorbonne Université, Université Paris Cité , 24 rue Lhomond, 75231 Paris Cedex 05, France.*

C'est trop bien

Intro

Fig. 2 shows the change in photoluminescence (PL) with respect to an external magnetic field for two samples with a low and high concentration of NV$^-$ centers. Both samples show a decrease in PL as the magnetic field amplitude increases, due to eigenstate mixing caused by the transverse part of the magnetic field [5, 13]. We notice however a stark difference in the low magnetic field region where only the high-density sample observe a drop in PL. In this article we propose to explore the reasons behind this zero-field line present only for dense NV$^-$ ensemble.

Unlike the decrease in PL for higher magnetic field values, the drop in PL at low magnetic field is associated with a decrease of the NV's spin lifetime T_1. Indeed, since the $|m_s = 0\rangle$ spin state is brighter than the $|m_s = \pm 1\rangle$ states, and since the optical pumping in the $|m_s = 0\rangle$ state is in competition with the relaxation in a thermal distribution of the states, decreasing the spins lifetime results in a decrease of the NV PL [8]. To understand the behavior of the PL in zero-field, we therefore need to study the dynamics of the spin in the low magnetic field region.

The T_1 depolarization dynamics of single or dilute NV centers at room temperature is dominated by a two-phonon Raman process [11, 16, 20], which depends on the crystal lattice temperature but does not depend on the external magnetic field. However, it has been observed

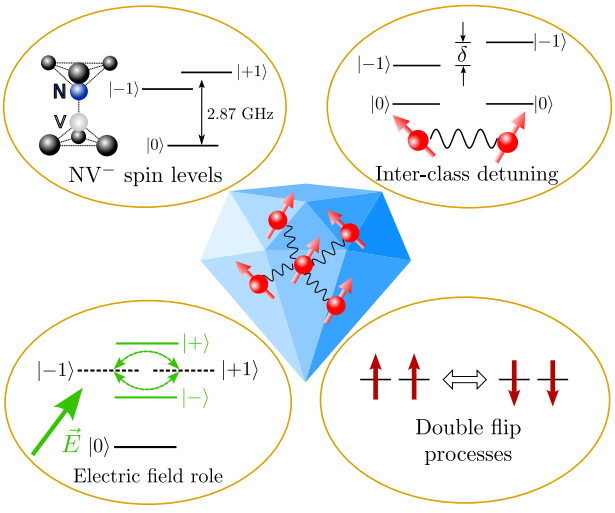

FIG. 1. Shema

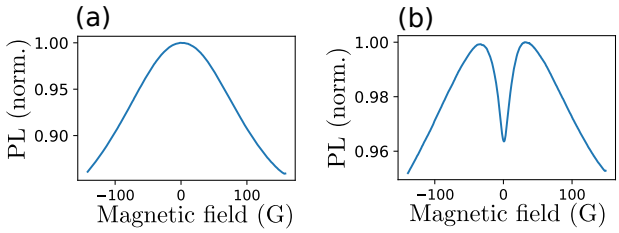

FIG. 2. Photoluminescence measurement from NV centers ensemble as a function of an external magnetic field randomly oriented (a) for a CVD sample containing ≈ 4 ppb NV$^-$ centers, (b) for an HPHT sample containing ≈ 3 ppm NV$^-$ centers

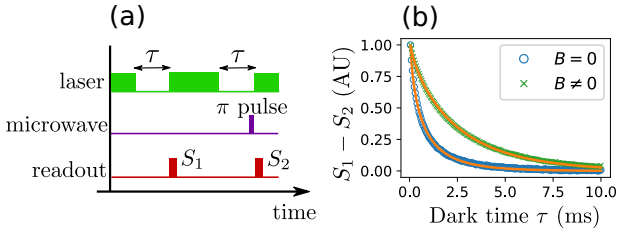

FIG. 3. Spin T_1 measurement protocol. (a) Sequence used to measure the spin lifetime : the laser is turned off for a time τ twice and the spin state is read at the end of the dark time by measuring the initial photoluminescence when the laser is turned back on. A microwave π-pulse resonant with one of the spin transition is placed before the second reading. The T_1 sequence result is the subtraction $S_1 - S_2$. (b) Measurement of $S_1 - S_2$ for a high density of NV centers in zero magnetic field field and non-zero magnetic field. The fit (orange plain line) is detailed in the main text

that dense NV centers ensemble have an additional spin decay channel [1–3, 11, 12, 14, 15, 17], which depends greatly on the magnetic field and not on the temperature . This effect has been attributed to cross-relaxation between the NV centers through dipole-dipole coupling [3, 15]. Some inhomogeneity between the NV centers is further needed in order to explain the depolarization of the spin ensemble. We will denote T_1^{ph} the characteristic time associated with the phonon relaxation process and T_1^{dd} the characteristic time associated with the dipole-dipole relaxation process.

The spin lifetime protocol used here is described in Fig. 3 and is based on previous similar experiments [3, 11, 15]. It consists in a pump-probe measurement where the spins are first polarized in the $|0\rangle$ state by a green

laser, and read-out optically after a variable dark time τ. Using only this sequence can result in artifacts in the signal, mostly due to charge state transfer in the dark [9, 10]. It is therefore convenient to repeat the sequence with an additional π pulse right before the spin read-out to project the remaining $|0\rangle$ polarization into a darker $|+1\rangle$ or $|-1\rangle$ state. By subtracting the result of the two sequences, we select only the spin-dependent part of the signal, with the added benefit of being able to select a specific class of NV centers.

The ensemble spin decay is non-exponential due to inhomogeneities between the NV^- centers. We will base our interpretations of the experimental results on the NV-fluctuator model developed in [3]. A conclusion of this model is that, for an homogeneous 3D distribution of fluctuator, the dipole-induced lifetime should be stretched-exponential with a stretch factor $\beta = 1/2$. Such an ensemble lifetime is indeed observed when $T_1^{\mathrm{dd}} \ll T_1^{\mathrm{ph}}$ (see SI).

For the samples used in this paper (detailed in SI), we observed that $T_1^{\mathrm{dd}} \sim T_1^{\mathrm{ph}}$, meaning that we had to include both in our analysis. The resulting fitting formula is therefore :

$$S(\tau) = A \exp\left(-\frac{\tau}{T_1^{\mathrm{ph}}} - \sqrt{\frac{\tau}{T_1^{\mathrm{dd}}}}\right), \qquad (1)$$

Further details on the fitting procedure are available in SI. For the rest of the article we will be only interested on the stretched exponential lifetime T_1^{dd}.

One of the way we can isolate dipole-dipole related phenomena with NV centers is by tuning the number of NV centers resonant with each other. Indeed, Fig. 4 (bi) shows the characteristic 8 lines observed with ensemble NV optically detected magnetic resonance (ODMR) spectrum. These 8 lines correspond to the four "classes" of NV centers - that is physical orientation of the NV axis is the diamond crystal cell - multiplied by the two possible spin transitions $|0\rangle \rightarrow |-1\rangle$ and $|0\rangle \rightarrow |+1\rangle$. The transitions of the four different classes can be controlled somewhat independently by changing the amplitude and orientation of the external magnetic field, and in particular they can be brought to resonance for particular orientation of the magnetic field. Fig. 4 (ci) shows an example where all four classes are brought to resonance by placing the magnetic field along the [100] crystalline axis. Other example of class resonance are given in SI.

Fig. 4 (bii) and (biii) shows respectively the PL and the stretched exponential spin decay T_1^{dd} of an ensemble of NV centers with respect to the amplitude of the external magnetic field. The orientation of the magnetic field was chosen in order to lift the degeneracy between the four classes, as shown in Fig. 4 (bi). We observe that the drop in PL at low magnetic field is indeed correlated with an increase in the spin decay rate, as is expected due to the higher number of resonant spins in zero magnetic field, where all four classes are resonant, compared to the non-degenerate case for $\vec{\neq}0$. We can also see that the decrease in PL for $B > 40$ G due to state mixing by the transverse magnetic field is not correlated to a modification of the spin lifetime.

However, the splitting of the four classes is not sole reason to the decrease of the spin lifetime in low magnetic field. Indeed, we performed similar measurements in Fig. 4 (cii) and (ciii) but this time fixing the magnetic field orientation along the [100] axis. For this particular orientation, the four classes are always resonant, regardless of the field amplitude. We can see that, although considerably reduced, there still is an increase in the spin decay rate and a corresponding drop in PL for low magnetic field values. We attribute the slight drop in PL and the corresponding bump for $1/T_1^{\mathrm{dd}}$ at $B \sim 20$ G to dipolar interaction with NV having a first neighbor ^{13}C [18].

The aim of this paper is to understand the remaining contribution to the spin decay in this second case. We identified and isolated two additional effects : the domination by the local electric field for low magnetic field value which results in a change of the spin Hamiltonian eigenstates, and the presence of double-flip processes where both NV spins involved in the dipole-dipole coupling flip their spin in the same direction.

In order to distinguish these two contributions, we decided to simulate the effect of the electric field by using a transverse magnetic field : for relatively weak transverse magnetic field, the eigen basis of the spin Hamiltonian is close to $\{|0\rangle, |+\rangle = \frac{|+1\rangle+|-1\rangle}{\sqrt{2}}, |-\rangle = \frac{|+1\rangle-|-1\rangle}{\sqrt{2}}\}$, which is the the spin Hamiltonian basis when the electric field dominates, as detailed in SI. This property has been used to observe a linear dependence in the electric field for the spin transition frequencies by applying an external transverse magnetic field [4, 19].

Fig. 5 (a) shows the energy levels for the three eigenstates of the NV spin Hamiltonian with respect to a purely transverse magnetic field. We will denote these eigenstates in the general case $|g\rangle$, $|d\rangle$ and $|e\rangle$. For weak transverse magnetic field, $|g\rangle \approx |0\rangle$, $|d\rangle = |-\rangle$ and $|e\rangle \approx |+\rangle$. As the magnetic field increases, $|g\rangle$ and $|e\rangle$ starts to become a mixing of $|0\rangle$ and $|+\rangle$ while $|d\rangle$ remains equal to $|-\rangle$.

Crucially, this mixing happens on a different scale than the associated energy splitting of the $|d\rangle$ and $|e\rangle$ states : Fig. 5 (b) shows both the splitting between the energy levels of $|d\rangle$ and $|e\rangle$, and the matching factor $|\langle e|+\rangle|^2$ characterizing the closeness of the states $\langle e|$ and $\langle +|$. We can see that for a field value of $\sim 130G$, the splitting between the $|d\rangle$ and $|e\rangle$ reaches $\sim 50MHz$, far exceeding the range of the dipole-dipole resonant coupling (see details in SI), but $|\langle e|+\rangle|^2 > 0.98$ meaning that the spin Hamiltonian eigenstates are still roughly in the $|0\rangle, |+\rangle, |-\rangle$ basis. We can therefore decouple the effects of the double-flip processes, which are no longer resonant, from the effects of the change of basis induced by the transverse electric - or in this case magnetic - field.

Fig. 5 (c) shows the measurement of the stretched lifetime T_1^{dd} for a single class of NV centers exposed to a transverse magnetic field between 25 and 130 G. The

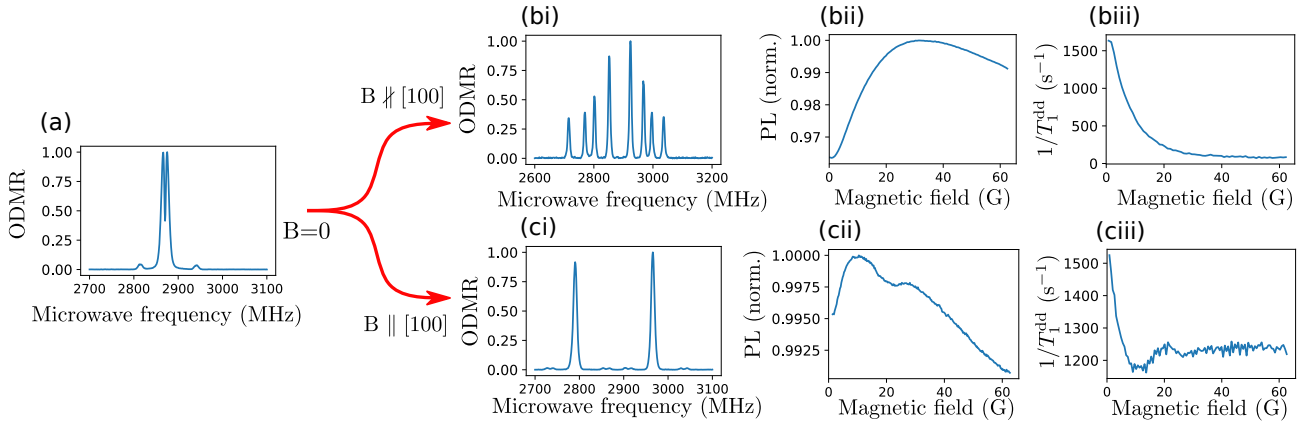

FIG. 4. Dependency on the magnetic field angle for the zero field depolarization. (a) ODMR spectrum in zero field. (bi) ODMR spectrum for a magnetic field ≈ 60 G, misaligned by $\sim 24°$ with the [100] axis. (bii) Normalized photoluminescence of the NV^- ensemble as a function of the magnetic field amplitude. (biii) Stretch part of the spin decay $1/T_1^{dd}$ as a function of the magnetic field amplitude. (ci), (cii) and (ciii) : same measurement with a magnetic field aligned with the [100] axis

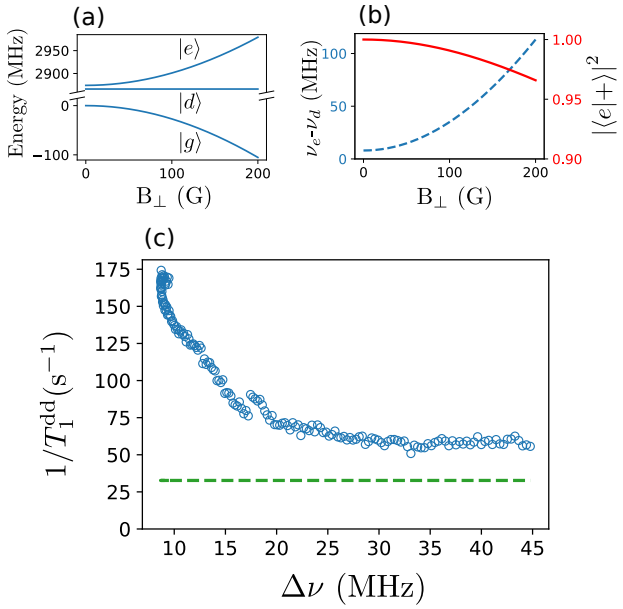

FIG. 5. (a) Simulated energies for the spin Hamiltonian in the presence of pure transverse magnetic field $B_\perp$. The three spin levels are denoted $|g\rangle$, $|d\rangle$ and $|e\rangle$. (b) Blue dashed curve : frequency detuning $\Delta\nu$ between the $|g\rangle$, $|d\rangle$ states. Red plain curve : Matching factor $|\langle e|+\rangle|^2$ between the states $\langle e|$ and $\langle +|$. (c) Measurement of the stretched exponential decay rate $1/T_1^{dd}$ for a single class as a function of the measured detuning $\Delta\nu$ between the two transitions $|g\rangle \rightarrow |d\rangle$ and $|g\rangle \rightarrow |e\rangle$ for purely transverse magnetic field. The green dashed line correspond to the decay rate for the same class when the magnetic field is longitudinal

detuning $\Delta\nu$ between the two states $|d\rangle$ and $|e\rangle$ was measured through ODMR. We attribute the decrease in the spin decay rate when the detuning increases to the loss of effectiveness of the double-flip processes. We can notice that the decay rate reaches a plateau for $\Delta\nu \geq 30$ MHz with a value about twice as big as the decay rate for a longitudinal magnetic field. This plateau we attribute to the effect of the transverse magnetic field, which we assume to be similar to the effect of the electric field in the low magnetic field regime. We should note that the effect of the double-flip processes is about 4 times more important in the depolarization rate than the effect of the electric field, even though the states are not initially fully resonant.

Overall we predicted, based on an extension of the fluctuator model developed in SI, an increase by a factor of $\sim$ 4 of the dipole-dipole induced decay rate in the non-magnetic basis $|0\rangle, |+\rangle, |-\rangle$ compared to the magnetic basis $|0\rangle, |+1\rangle, |-1\rangle$. While the measured increase is smaller than the predicted one, as with most of the predictions based on the fluctuator model, the measurements agrees with the theoretical increase in the flip-flop rate in the $|+/-\rangle$ basis compared to the $|\pm 1\rangle$ basis.

Similarly, we can compute the predicted decay rate in the $\vec{B} \parallel [100]$ case compared to the $\vec{B} = 0$ case, and find a theoretical increase of $\sim 20\%$ in the $\vec{B} = 0$ case due to the effects of the local electric field. This, along with the double-flip processes explains the behavior observed in Fig. 4 (cii) and (ciii).

MAGNETOMETRY

DC microwave-less magnetometry has already been performed with NV ensembles, using either NV-NV cross-relaxations [1, 2] or level anti-crossing [21–23]. Here we propose to perform a similar protocol, but using the spin depolarization in zero-field. The main difference with the previously mentioned protocols is the fact that this one doesn't rely on crystalline orientation, making this protocol usable with diamond powders or polycrystalline samples. The idea of performing optical magnetometry on the zero-field photoluminescence feature of

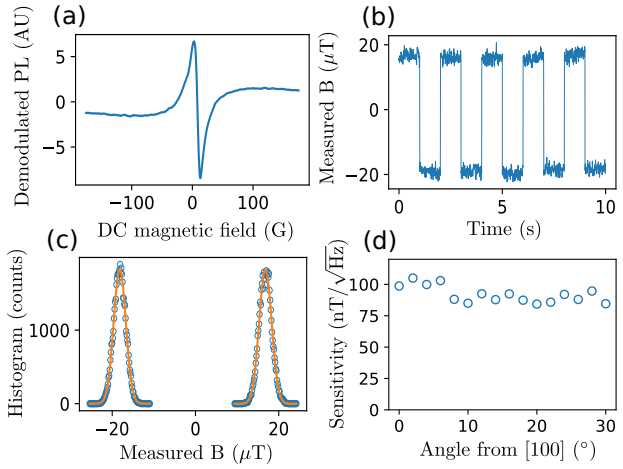

FIG. 6. Low field magnetometry protocol. (a) Demodulated photoluminescence as a function of an externally applied magnetic field with an additional oscillatory magnetic field. (b) Measured magnetic field when alternating a small external magnetic field offset. (c) Histogram of the measurement in Fig. (b) fitted with gaussians of standard deviation $\sigma = 1.5$ μT. (d) Measured sensitivity as function of the angle between the external magnetic field and the [100] crystalline axis.

NV ensembles has been suggested before [6, 7] but had not been implemented so far.

Fig. 6 (a) shows the demodulated PL when a DC magnetic field is scanned in a random direction and an additional alternating magnetic field of a few Gauss at $\sim$ kHz is added through the same electromagnet (see experimental details in SI). We can see a sharp and relatively linear slope in low field $|B| < 5$ G. Once calibrated, in this case with ODMR, the slope can provide a 1D magnetic field measurement, which could be extended to 3D with a set of 3 coils or 3 electromagnets, as seen in [23].

In order to measure the sensitivity of the measurement, we alternate a small DC field of ≈ 40 μT every few seconds and take an histogram of the measured fields, as shown in Fig. 6 (b) and (c). The histogram is well fitted with gaussians of standard deviation $\sigma = 1.5$ μT. The measurement was performed here with an output low-pass filter of time constant $\tau = 3$ ms, which allows us to measure the sensitivity $\eta = \sigma\sqrt{\tau} = 82$ nT$/\sqrt{\text{Hz}}$.

We can then try to measure the relative importance of the three causes of spin depolarization on the field sensitivity, namely the splitting of the classes, the local electric field and the double-flip processes. In order to do so, we measure the sensitivity while changing the angle of the field. When $\vec{B}$ is aligned with the [100] crystalline axis, only the double flips and the electric field cause a depolarization, whereas in every other orientation the three effects are at play.

The results are shown in Fig. 6 (d). We can see a slight increase of $\sim 10\%$ in the sensitivity as we leave the [100] region, but overall the sensitivity remains relatively flat, which means that the double-flips and electric field effects are the dominant factors in the sensitivity of this protocol. While it may seem surprising that the effects with a lower contribution on the PL contrast have a higher effect on this PL-based protocol, what matters here is not the absolute contrast but the slope of the change of contrast with respect to the magnetic field, which is sharper for the electric field and double flips than it is for the lift of degeneracy. It should be noted though that this observation is sample dependent, and that other samples, including from the same batch, have shown a higher orientation dependence, corresponding to a lower contribution from the electric field and double-flip processes.

CONCLUSION

In this work we have identified three mechanisms causing the extra spin depolarization observed in zero field for dense ensemble of NV$^-$ centers, all related to an increase in the dipole-dipole cross-relaxations between the spins : the lift of degeneracy between the four classes caused by the magnetic field, the domination of the local electric field which causes a change in the Hamiltonian eigenstates, and the double-flip process allowed by the proximity in energy of the spin $|\pm\rangle$ states. We identified the lift in degeneracy as the main cause in the zero-field depolarization, followed by the double-flip processes and then the electric field. We have demonstrated a potential use of this depolarization as a DC microwave-less and orientation-free magnetometer with sensitivity below 100 nm$/\sqrt{\text{Hz}}$ for a single 10 μm crystal.We have observed that in some cases the double-flips and electric field play a more important role than the lift of degeneracy in the magnetometry sensitivity.

ACKNOWLEDGEMENTS

[1] Rinat Akhmedzhanov, Lev Gushchin, Nikolay Nizov, Vladimir Nizov, Dmitry Sobgayda, Ilya Zelensky, and Philip Hemmer. Microwave-free magnetometry based on cross-relaxation resonances in diamond nitrogen-vacancy centers. *Phys. Rev. A*, 96(1):013806, July 2017. Number: 1.

[2] Rinat Akhmedzhanov, Lev Gushchin, Nikolay Nizov, Vladimir Nizov, Dmitry Sobgayda, Ilya Zelensky, and Philip Hemmer. Magnetometry by cross-relaxation-resonance detection in ensembles of nitrogen-vacancy centers. *Phys. Rev. A*, 100(4):043844, October 2019. Number: 4.

[3] Joonhee Choi, Soonwon Choi, Georg Kucsko, Peter C. Maurer, Brendan J. Shields, Hitoshi Sumiya, Shinobu Onoda, Junichi Isoya, Eugene Demler, Fedor Jelezko, Norman Y. Yao, and Mikhail D. Lukin. Depolarization Dynamics in a Strongly Interacting Solid-State Spin Ensemble. *Phys. Rev. Lett.*, 118(9):093601, March 2017. Number: 9.

[4] Florian Dolde, Helmut Fedder, Marcus W Doherty, Tobias Nöbauer, Florian Rempp, Gopalakrishnan Balasubramanian, Thomas Wolf, Friedemann Reinhard, Lloyd CL Hollenberg, Fedor Jelezko, et al. Electric-field sensing using single diamond spins. *Nature Physics*, 7(6):459–463, 2011.

[5] RJ Epstein, FM Mendoza, YK Kato, and DD Awschalom. Anisotropic interactions of a single spin and dark-spin spectroscopy in diamond. *Nature physics*, 1(2):94–98, 2005.

[6] DS Filimonenko, VM Yasinskii, Alexander P Nizovtsev, S Ya Kilin, and Fedor Jelezko. Manifestation in irluminescence of cross relaxation processes between nv-centers in weak magnetic fields. *Journal of Applied Spectroscopy*, 88(6):1131–1143, 2022.

[7] DS Filimonenko, VM Yasinskii, AP Nizovtsev, and S Ya Kilin. Weak magnetic field resonance effects in diamond with nitrogen-vacancy centers. *Semiconductors*, 52(14):1865–1867, 2018.

[8] Aurore Finco, Angela Haykal, Rana Tanos, Florentin Fabre, Saddem Chouaieb, Waseem Akhtar, Isabelle Robert-Philip, William Legrand, Fernando Ajejas, Karim Bouzehouane, et al. Imaging non-collinear antiferromagnetic textures via single spin relaxometry. *Nature communications*, 12(1):1–6, 2021.

[9] R. Giri, C. Dorigoni, S. Tambalo, F. Gorrini, and A. Bifone. Selective measurement of charge dynamics in an ensemble of nitrogen-vacancy centers in nanodiamond and bulk diamond. *Phys. Rev. B*, 99(15):155426, April 2019. Number: 15.

[10] R. Giri, F. Gorrini, C. Dorigoni, C. E. Avalos, M. Cazzanelli, S. Tambalo, and A. Bifone. Coupled charge and spin dynamics in high-density ensembles of nitrogen-vacancy centers in diamond. *Phys. Rev. B*, 98(4):045401, July 2018. Number: 4.

[11] A. Jarmola, V. M. Acosta, K. Jensen, S. Chemerisov, and D. Budker. Temperature- and Magnetic-Field-Dependent Longitudinal Spin Relaxation in Nitrogen-Vacancy Ensembles in Diamond. *Phys. Rev. Lett.*, 108(19):197601, May 2012. Number: 19.

[12] A. Jarmola, A. Berzins, J. Smits, K. Smits, J. Prikulis, F. Gahbauer, R. Ferber, D. Erts, M. Auzinsh, and D. Budker. Longitudinal spin-relaxation in nitrogen-vacancy centers in electron irradiated diamond. *Appl. Phys. Lett.*, 107(24):242403, December 2015. Number: 24.

[13] Ngoc Diep Lai, Dingwei Zheng, Fedor Jelezko, François Treussart, and Jean-François Roch. Influence of a static magnetic field on the photoluminescence of an ensemble of nitrogen-vacancy color centers in a diamond single-crystal. *Applied Physics Letters*, 95(13):133101, 2009.

[14] Mariusz Mrózek, Adam M Wojciechowski, and Wojciech Gawlik. Characterization of strong nv- gradient in the e-beam irradiated diamond sample. *Diamond and Related Materials*, 120:108689, 2021.

[15] Mariusz Mrózek, Daniel Rudnicki, Pauli Kehayias, Andrey Jarmola, Dmitry Budker, and Wojciech Gawlik. Longitudinal spin relaxation in nitrogen-vacancy ensembles in diamond. *EPJ Quantum Technol.*, 2(1):22, December 2015. Number: 1.

[16] A Norambuena, E Muñoz, HT Dinani, A Jarmola, Patrick Maletinsky, Dmitry Budker, and JR Maze. Spin-lattice relaxation of individual solid-state spins. *Physical Review B*, 97(9):094304, 2018.

[17] C Pellet-Mary, P Huillery, M Perdriat, and G Hétet. Magnetic torque enhanced by tunable dipolar interactions. *Physical Review B*, 104(10):L100411, 2021.

[18] Clément Pellet-Mary, Paul Huillery, Maxime Perdriat, A Tallaire, and Gabriel Hétet. Optical detection of paramagnetic defects in diamond grown by chemical vapor deposition. *Physical Review B*, 103(10):L100411, 2021.

[19] Ziwei Qiu, Assaf Hamo, Uri Vool, Tony X Zhou, and Amir Yacoby. Nanoscale electric field imaging with an ambient scanning quantum sensor microscope. *arXiv preprint arXiv:2205.03952*, 2022.

[20] DA Redman, S Brown, RH Sands, and SC Rand. Spin dynamics and electronic states of n-v centers in diamond by epr and four-wave-mixing spectroscopy. *Physical review letters*, 67(24):3420, 1991.

[21] Arne Wickenbrock, Huijie Zheng, Lykourgos Bougas, Nathan Leefer, Samer Afach, Andrey Jarmola, Victor M. Acosta, and Dmitry Budker. Microwave-free magnetometry with nitrogen-vacancy centers in diamond. *Applied Physics Letters*, 109(5):053505, 2016.

[22] Huijie Zheng, Georgios Chatzidrosos, Arne Wickenbrock, Lykourgos Bougas, Reinis Lazda, Andris Berzins, Florian Helmuth Gahbauer, Marcis Auzinsh, Ruvin Ferber, and Dmitry Budker. Level anti-crossing magnetometry with color centers in diamond. In *Slow Light, Fast Light, and Opto-Atomic Precision Metrology X*, volume 10119, pages 115–122. SPIE, 2017.

[23] Huijie Zheng, Zhiyin Sun, Georgios Chatzidrosos, Chen Zhang, Kazuo Nakamura, Hitoshi Sumiya, Takeshi Ohshima, Junichi Isoya, Jörg Wrachtrup, Arne Wickenbrock, and Dmitry Budker. Microwave-Free Vector Magnetometry with Nitrogen-Vacancy Centers along a Single Axis in Diamond. *Phys. Rev. Applied*, 13(4):044023, April 2020. Number: 4.